Mathematical modeling

Математическое моделирование

UDC 621.396.969.1
https://doi.org/10.32362/2500-316X-2024-12-3-65-77
EDN TUXBXL

RESEARCH ARTICLE

High-resolution 2D-DoA sequential algorithm of azimuth and elevation estimation in automotive distributed system of coherent MIMO radars

Igor V. Artyukhin @

Lobachevsky State University of Nizhny Novgorod, Nizhny Novgorod, 603950 Russia
@ *Corresponding author, e-mail: artjukhin@rf.unn.ru*

Abstract

Objectives. One of the main tasks of radiolocation involves the problem of increasing spatial resolution of the targets in the case of limited aperture of the radar antenna array and short length of time samples (snapshots). Algorithms must be developed to provide high angular resolution and low computational complexity. In order to conform with the existing Advanced Driver Assistance Systems requirements, modern cars are equipped with more than one radar having a common signal processing scheme to improve performance during target detection, positioning, and recognition as compared to a single radar. The present study aims to develop a two-dimensional Direction-of-Arrival algorithm with low computation complexity as part of distributed coherent automotive radar system for cases involving short time samples (snapshots).

Methods. A virtual antenna array formation algorithm is formulated according to the two-dimensional Capon method. A proposed modification of two-dimensional Capon algorithm is based on sequentially estimating the directions of arrival for the distributed radar system. The Monte Carlo method is used to compare the effectiveness of the considered algorithms.

Results. The 2D-DoA sequential algorithm of azimuth and elevation estimation is proposed. The comparative analysis results for the developed algorithm and classical 2D Capon method based on numerical simulation using Monte Carlo method are presented. The proposed scheme of DoA estimation for coherent signal processing of distributed radars is shown to lead to an improvement of the main considered metrics representing the probability of correctly estimating the number of targets, mean square error, and square error compared to a single radar system. The proposed low-computational algorithm shows the gain in complexity compared to full 2D Capon algorithm.

Conclusions. The proposed two-stage algorithm for estimating the directions of arrival of signals in azimuth and elevation planes can be applied to the distributed system of coherent radars with several receiving and transmitting antennas representing multiple input multiple output (MIMO) radars. The algorithm is based on sequentially estimating the directions of arrival, implying estimation in the azimuthal plane at the first stage and estimation in the vertical plane at the second stage. The performance of a coherent radar system with limited antenna array configuration of separate radar is close in characteristics to a high-performance 4D-radar with a large antenna array system.

Keywords: automotive distributed radars, coherent signal processing, high-resolution algorithms, 2D Capon algorithm

• **Submitted:** 18.07.2023 • **Revised:** 18.03.2024 • **Accepted:** 05.04.2024

For citation: Artyukhin I.V. High-resolution 2D-DOA sequential algorithm of azimuth and elevation estimation in automotive distributed system of coherent MIMO radars. *Russ. Technol. J.* 2024;12(3):65–77. https://doi.org/10.32362/2500-316X-2024-12-3-65-77

Financial disclosure: The author has no a financial or property interest in any material or method mentioned.

The author declares no conflicts of interest.

НАУЧНАЯ СТАТЬЯ

Двумерный алгоритм с последовательной оценкой углов прихода сигналов в системе когерентных распределенных автомобильных радаров с несколькими приемными и передающими антеннами

И.В. Артюхин @

Нижегородский государственный университет им. Н.И. Лобачевского, Нижний Новгород, 603950 Россия
@ *Автор для переписки, e-mail: artjukhin@rf.unn.ru*

Резюме

Цели. Одной из актуальных задач в радиолокации является проблема повышения пространственного разрешения целей при ограниченной апертуре антенной решетки радара и короткой выборке входных отсчетов. Разрабатываемые алгоритмы должны обеспечивать высокое угловое разрешение и иметь малую вычислительную сложность. В настоящее время автомобили для выполнения требований систем безопасности и помощи водителю оснащаются не одним, а несколькими радарами с общей схемой обработки сигналов для улучшения характеристик при обнаружении, позиционировании и распознавании целей по сравнению с одиночным радаром. Цель работы – разработка двумерного алгоритма оценки угловых координат с низкой вычислительной сложностью в системе распределенных когерентных автомобильных радаров для случая короткой выборки входных отсчетов.

Методы. Использованы алгоритм формирования виртуальной антенной решетки, двумерный метод Кейпона. Предложена модификация метода Кейпона на основе последовательной оценки углов прихода сигналов применительно к системе распределенных радаров. Для сравнения эффективности рассматриваемых алгоритмов используется метод Монте-Карло.

Результаты. Представлен алгоритм с последовательной оценкой азимута и угла места для системы распределенных когерентных автомобильных радаров. Приведены результаты сравнительного анализа предложенного алгоритма и классического двумерного метода Кейпона на основе численного моделирования при помощи метода Монте-Карло. Показано, что предложенная схема приводит к улучшению целевых метрик (вероятности правильного определения числа целей, среднеквадратической и систематической ошибок измерения азимута и угла места) по сравнению с одиночным радаром. Последовательный алгоритм обеспечивает выигрыш в использовании вычислительных ресурсов по сравнению с полным двумерным методом Кейпона.

Выводы. Предложенный двумерный метод оценки углов прихода сигналов в азимутальной и угломестной плоскостях может быть применен для распределенной системы бистатических когерентных радаров с несколькими приемными и передающими антеннами (MIMO-радаров). Метод основан на последовательной оценке углов прихода (на первом шаге – в азимутальной плоскости, на втором – в вертикальной). Характеристики системы когерентных радаров с ограниченной конфигурацией антенной решетки, сравнимы с характеристиками высокопроизводительного 4D-радара со значительно большим числом элементов антенной решетки.

Ключевые слова: распределенные автомобильные радары, когерентная обработка, алгоритмы сверхразрешения, двумерный алгоритм Кейпона

• **Поступила:** 18.07.2023 • **Доработана:** 18.03.2024 • **Принята к опубликованию:** 05.04.2024

Для цитирования: Артюхин И.В. Двумерный алгоритм с последовательной оценкой углов прихода сигналов в системе когерентных распределенных автомобильных радаров с несколькими приемными и передающими антеннами. *Russ. Technol. J*. 2024;12(3):65–77. https://doi.org/10.32362/2500-316X-2024-12-3-65-77

Прозрачность финансовой деятельности: Автор не имеет финансовой заинтересованности в представленных материалах или методах.

Автор заявляет об отсутствии конфликта интересов.

INTRODUCTION

Recent developments in the field of automotive electronics have given rise to a new generation of radars called 4D radars[1]. Such devices allow simultaneous measurement of three spatial coordinates (distance, azimuth, and elevation) and velocity (Doppler shift). At the same time, the high spatial resolution enables recognition of overlapping images, such as a pedestrian standing by a fence or a motorcycle driving next to a truck.

One way to improve angular resolution is to increase the number of transmitters (Tx) and receivers (Rx). However, this approach is limited by the complexity of hardware implementation and high cost of the final product. Currently, the number of antennas ranges from a few units to several dozen per radar. For example, the Continental ARS540 radar (Xilinx, Germany) is equipped with 12 transmitters and 16 receivers[2]. The S80 automotive radar released by Uhnder, USA, has a similar configuration [1]. In the more advanced Phoenix radar by Arbe (Israel)[3], up to 48 Tx and 48 Rx are implemented.

Given the limitation on the number of physical antennas, the angular resolution can be improved through applying additional high-resolution (HR) methods for neighboring signal sources (targets). Among classical HR algorithms, mention multiple signal classification (MUSIC), estimation of signal parameters via rotational invariant techniques (ESPRIT), Capon method, minimum polynomial method, and their variations [2–6] should be distinguished. However, these methods, while highly efficient, require large computational resources, especially when using antenna array systems (AAS) with a sufficiently large number of antennas.

In practice, when processing signals in automotive radars, the estimation of direction of arrival (DoA) is typically performed using only one sequence of short pulses (the so-called "frame"), which gives one snapshot (a time sample) in each radar [3, 7]. Thus, for the considered problem, the number of time samples is less than the number of AAS elements (the so-called "short sample"), resulting in the complexity of using the above-mentioned HR methods associated with the inversion of the ill-conditioned correlation matrix of such short input process.

The second technique for increasing angular resolution is based on implementing a coherent radar with multiple receiving and transmitting channels known as the multiple-input multiple-output (MIMO) radar. MIMO radars equipped with N_{Tx} Tx and N_{Rx} Rx antennas form a virtual AAS equivalent to that of a traditional system equipped with a single Tx antenna and $N_{\text{Tx}} \times N_{\text{Rx}}$ Rx antennas (called multiple-input single-output (MISO) radars). Thus, MIMO radars provide an efficient path to achieve high angular resolution with fewer real antennas [7–9]. However, they require all received signals to be coherent and that the waveform be orthogonal. When constructing MIMO radars, different orthogonalization methods are used, such as time or code division of signals [8, 9].

Using the MIMO technology, Arbe's Phoenix radar can create up to 2304 virtual antennas providing an angular resolution (3 dB beamwidth of antenna pattern) of 1.25° and 1.5° in azimuth and elevation, respectively. At the same time, the field of view (FoV) is ±60° in the azimuth plane and ±15° in elevation. Following the same approach, the Continental ARS540 radar can create 192 virtual antennas with 1.2° azimuth resolution and 2.3° elevation resolution.

In order to satisfy existing requirements of advanced driver assistance systems (ADAS), modern cars are equipped with several sensors capable of operating as a single unit and having a common (centralized) signal processing. The advantages of such systems include a significant improvement in their performance when solving detection-, positioning-, and target-recognition tasks as compared to a single radar (traditional or MIMO).

[1] https://autotech.news/the-future-of-automotive-radar-4d-imaging-radar/. Accessed February 07, 2024.

[2] https://www.xilinx.com/publications/presentations/continental-ARS540-powered-by-xilinx.pdf. Accessed August 21, 2023.

[3] https://arberobotics.com/wp-content/uploads/2021/04/4D_Imaging_Radar_Product_Overview.pdf. Accessed August 21, 2023.

Two approaches to integrating measurements from different radars are typically distinguished, based on coherent and incoherent signal processing. The incoherent scheme involves combining signals of single radars operating in monostatic mode [10, 11]. The coherent scheme is based on creating a joint virtual AAS of distributed radars operating in the bistatic measurement mode, which requires full or partial time/frequency synchronization of signals between radars [12].

The present paper considers the 2D DoA estimation method for coherent signal processing in the distributed automotive radar system (DRS) for short length of time samples. This method should provide high angular resolution by coherent signal processing in distributed radars with a small number of real antennas instead of using a single high-performance 4D radar with large AAS. At the same time, 1° azimuth resolution and 2° elevation are considered as necessary characteristics.

1. CREATING VIRTUAL AAS FOR DISTRIBUTED COHERENT RADAR SYSTEM

We consider a distributed system consisting of two coherent MIMO radars. Assume that this system has real N_{Tx} transmitters and N_{Rx} receivers. The total number of antennas of virtual AAS equals to $N_{\text{virt}} = N_{\text{Tx}} \cdot N_{\text{Rx}}$.

The location of virtual antennas is defined as the convolution of coordinates of real receivers and transmitters [13, 14]. The coordinates of the mth virtual antenna may be calculated from the following formula:

$$\boldsymbol{\rho}^{(m)} = \mathbf{r}_{\text{Tx}}^{(p)} + \mathbf{r}_{\text{Rx}}^{(q)} - \mathbf{r}_0, \qquad (1)$$

where $\mathbf{r}_{\text{Tx}}^{(p)}$ is the position vector of coordinates of the pth element of the transmitter; $\mathbf{r}_{\text{Rx}}^{(q)}$ is the position vector of coordinates of the qth element of the receiver; $\mathbf{r}_0$ is the position vector determining the choice of the coordinate system; $m = q \cdot p$. Here it should be noted that, under certain conditions of the radar AAS architecture, several virtual antennas can have similar space coordinates.

Thus, equation (1) can be rewritten in the following form:

$$\boldsymbol{\rho}^{(m)} = \mathbf{r}_{\text{Tx}}^{(p)} + \mathbf{r}_{\text{Rx}}^{(q)} - \mathbf{r}_{\text{Tx}}^{(1)} - \mathbf{r}_{\text{Rx}}^{(1)}, \qquad (2)$$

where $\mathbf{r}_{\text{Tx}}^{(1)}$ and $\mathbf{r}_{\text{Rx}}^{(1)}$ are the position vector of coordinates of the first transmitting and first receiving AAS elements, respectively.

The properties of the virtual AR can be controlled by changing coordinates of real Rx and Tx antennas. The selection of antenna position is generally aimed at obtaining a virtual array having a larger aperture, resulting in the improved angular resolution of close objects. At the same time, the concept of virtual AAS allows the application of traditional AAS processing (including HR algorithms) to estimate angular coordinates. The basic idea of virtual AAS is to match its output signal with that generated by some real AAS. Although such a match is unambiguous in free space, multipath propagation determines the optimal configuration of real AAS by considering matching criteria. It is shown in [14] that, in the presence of a reflected signal from the Earth, either all transmitters or all receivers should have the same height above the Earth's surface. The simplest form of such configuration for real transmitting and receiving antennas is the L-shaped AAS.

An example of virtual AAS configuration for the distributed system consisting of two coherent radars with the L-shaped AAS is shown in Fig. 1. Transmitters are marked with a cross, while receivers are marked with a circle. The AASs of single radars are arranged symmetrically with respect to the vertical axis (radar center).

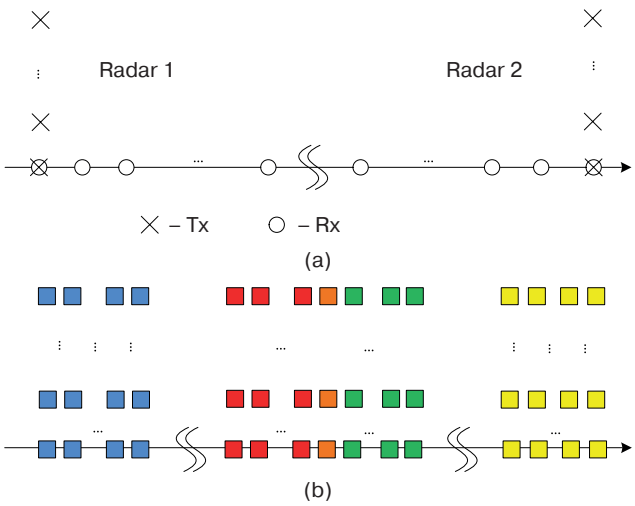

Fig. 1. General geometry of the distributed radar system: (a) AAS consisting of two L-type radars; (b) virtual AAS

The resulting virtual AAS consists of two virtual monostatic arrays (highlighted in blue and yellow colors in Fig. 1b) and one virtual bistatic array located in the middle. The bistatic AAS consists of twice the number of elements of the virtual single radar array [13, 14].

The virtual antennas formed using the bistatic response of the left radar are shown in red, while those of the right radar are shown in green. The middle elements highlighted in orange in the virtual AAS contain overlapping bistatic measurements from the right and left radars. This position of antennas in the middle column is necessary for considering and compensating for the phase difference occurring between bistatic signals in the virtual AAS under non-ideal time/frequency synchronization.

2. DESCRIPTION OF THE EXPLOITED ALGORITHMS

2.1. Phase compensation algorithm

We propose a signal phase compensation algorithm consisting of two stages. The first stage is used for non-zero installment angle α of single radars (Fig. 2). If the single radar installment angle is zero, then the first stage is skipped, and only the second stage is applied.

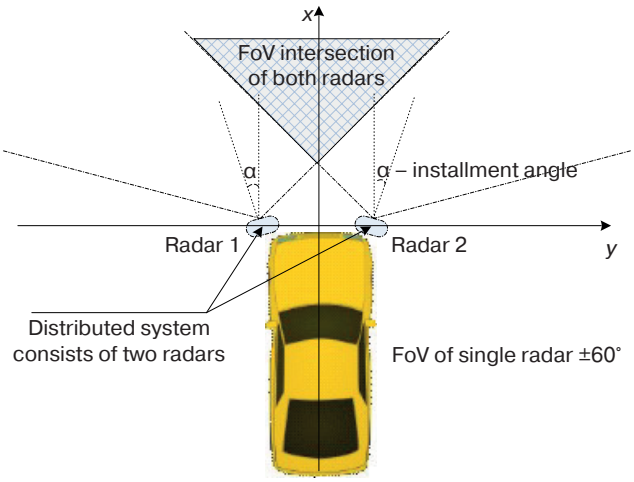

Fig. 2. General geometry of the distributed radar system. Top view

First stage: compensating for the additional phase incursion related to the non-zero installment angle of a single radar.

We denote the signals of virtual bistatic arrays (responses) from the left and right radars by matrices $\mathbf{Y}_i$ (i = 1, 2). We introduce the pth component of the AAS scanning vector $\mathbf{s}(\alpha)$ in azimuth for the radar installment angle α as follows:

$$s_p(\alpha) = \exp(2\pi j d_\lambda (p-1)\sin(\alpha)), \quad p = \overline{1,N}, \qquad (3)$$

where N is the number of antenna elements in the horizontal plane of a single radar, j is an imaginary unit.

In order to compensate for the additional phase incursion related to the non-zero installment angle of a single radar, the following transformation is performed:

$$\mathbf{Z}_1 = \mathbf{G}_1 \cdot \mathbf{Y}_1, \quad \mathbf{Z}_2 = \mathbf{G}_2 \cdot \mathbf{Y}_2, \qquad (4)$$

where

$$\mathbf{G}_1 = \mathbf{diag}\{\mathbf{s}\}, \mathbf{G}_2 = \mathbf{diag}\{\mathbf{s}^*\} \qquad (5)$$

and $\mathbf{diag}\{\mathbf{s}\}$ is a diagonal matrix, the elements of vector $\mathbf{s}$ lie on the main diagonal, and * is the sign of complex conjugation.

We introduce matrix $\mathbf{Z}$ of dimension $N_{Tx}/2 \times 2N$ containing signals $\mathbf{Z}_1$ and $\mathbf{Z}_2$:

$$\mathbf{Z} = [\mathbf{Z}_1, \mathbf{Z}_2]. \qquad (6)$$

Second stage: the jump in phases between bistatic radar measurements is compensated by taking into account the radar phase difference in the average element of the constructed virtual AAS.

We extract a separate row consisting of $2N$ elements: $\{z(1), z(2), \ldots z(2N)\}$ from the complete set $\mathbf{Z}$. The virtual antenna array (selected row) consists of $2N - 1$ elements with overlapping measurements in the middle element (Fig. 3).

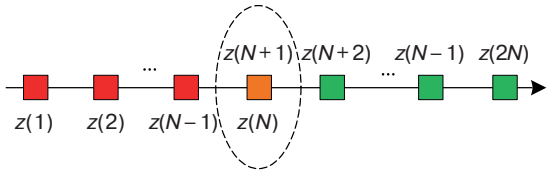

Fig. 3. Illustration of the sample construction for a separate row of the virtual array

We shall find the phase difference in the average element $\Delta\Phi = \text{phase}(z(N)) - \text{phase}(z(N+1))$ and compensate the obtained difference for antenna elements with indices $N + 2, \ldots, 2N$, as follows:

$$\{z(N+2), z(N+3), \ldots z(2N)\} \cdot \exp(-j \cdot \Delta\Phi). \qquad (7)$$

The transformed signals used to estimate DoA consist of the following $2N - 1$ elements:

$$\begin{aligned} &\{z(1), z(2), \ldots z(N),\ z(N+2) \cdot \exp(-j\Delta\Phi), \ldots \\ &z(N+3) \cdot \exp(-j\Delta\Phi), \ldots z(2N) \cdot \exp(-j\Delta\Phi)\}. \end{aligned} \qquad (8)$$

The element with index $N + 1$ from the complete set is not used in the final set (Fig. 4).

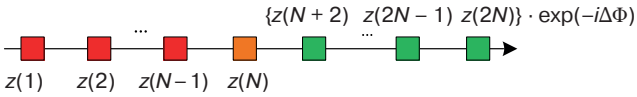

Fig. 4. Construction of samples for a separate row of the virtual array

2.2. Two-dimensional algorithm for estimating DoA

We consider two methods for estimating the azimuth and target elevation: the classical two-dimensional (2D) Capon algorithm and the proposed (new) two-step method for sequential estimation of azimuth and elevation.

The nonparametric 2D Capon method is selected as the basic approach. Although this method does not

require priori knowledge of the target quantity (or its prior estimation), which simplifies the DoA estimation, it has high computational complexity related to finding the inverse matrix and the two-dimensional search for extrema [2, 13]. This algorithm is based on the search for maxima of the two-dimensional resolution function $\eta_C(\varphi, \theta)$:

$$\eta_C(\varphi,\theta) = \frac{1}{\mathbf{S}(\varphi,\theta)^H \mathbf{M}_{2D}^{-1} \mathbf{S}(\varphi,\theta)}, \quad (9)$$

where $\mathbf{M}_{2D}$ is the estimation of the correlation matrix of the input process of the two-dimensional AAS, while $\mathbf{S}(\varphi, \theta)$ is the corresponding scanning vector.

The DoA estimation method proposed in the paper consists in the sequential estimation of azimuth (first step) and elevation (second step). We consider the proposed DoA estimation scheme in detail.

The first step involves implementing the one-dimensional Capon algorithm. Let there be an $m \times n$ virtual AAS (marked with blue squares in Fig. 5 on the left). A single time sample is used for estimating DoA, which can be represented mathematically using matrix $\mathbf{A}$ (see Fig. 5 on the right).

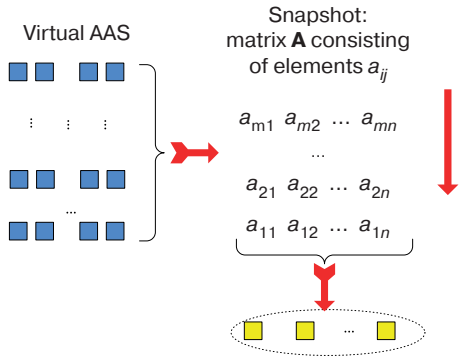

Fig. 5. Example of constructing samples for estimation in the azimuth plane

We select a horizontal row of length n (one-dimensional AAS is yellow squares marked with an ellipse in Fig. 5) from full virtual AAS. In this case, the entire matrix $\mathbf{A}$ is used to estimate the correlation matrix of one-dimensional AAS. Single rows of matrix $\mathbf{A}$ can be interpreted as "time samples" for one-dimensional AAS. We compile matrix $\mathbf{A}$ in the following form:

$$\mathbf{A} = \begin{bmatrix} a_{11} & a_{21} & \dots & a_{m1} \\ a_{12} & a_{22} & \dots & a_{m2} \\ \dots & \dots & \dots & \dots \\ a_{1n} & a_{2n} & \dots & a_{mn} \end{bmatrix}, \quad (10)$$

allowing the one-dimensional resolution function for the Capon method to be represented as the following expression:

$$\eta(\varphi) = \frac{1}{\mathbf{S}(\varphi)^H \mathbf{M}_{1D}^{-1} \mathbf{S}(\varphi)}, \quad (11)$$

where matrix $\mathbf{M}_{1D} = \frac{1}{L} \cdot \mathbf{A} \cdot \mathbf{A}^H$, $L = m$ is the number of rows in virtual AAS, $(\bullet)^H$ is Hermite conjugation.

Solving the maximization problem (11), we obtain k azimuth estimates: $\varphi_1, \dots, \varphi_k$.

In the second step, the 2D Capon algorithm for elevation estimation is implemented. However, unlike the full 2D Capon method, the search for maxima of resolution function $\eta_C(\varphi, \theta)$ is performed only at fixed values of the target azimuths $\varphi_1, \dots, \varphi_k$ found in the first step:

$$\eta_C(\varphi,\theta)\big|_{\varphi=\varphi_l} = \frac{1}{\mathbf{S}(\varphi,\theta)^H \mathbf{M}_{2D}^{-1} \mathbf{S}(\varphi,\theta)}\Bigg|_{\varphi=\varphi_l},$$

$$\varphi_l \text{ are fixed, } l = \overline{1,k}. \quad (12)$$

Thus, the problem of finding maxima for two-dimensional function $\eta_C(\varphi, \theta)$ (9) has been reduced to k one-dimensional hill-climbing problems (12). The solution to (12) is elevation estimates $\theta_1, \dots, \theta_k$.

The flowchart of the proposed algorithm is presented in Fig. 6.

2.3. Spatial smoothing procedure

In real-world problems, only a single snapshot is used to estimate DoAs. In this case, correlation matrices $\mathbf{M}_{1D}$ and $\mathbf{M}_{2D}$ are degenerate. For such situation, a spatial smoothing procedure for the input data is applied [3]. For this purpose, subarrays are selected in main AAS whose optimal size is $Q \approx 0.7N_{dim}$ [3, 5] for each N_{dim} dimension.

In order to explain the spatial smoothing procedure, the subarray formation on the example of the L-type radar system with 6T8R configuration is considered. Then the bistatic virtual array is 6×15 in size, and the size of subarray for spatial smoothing would be 4×10 when using the 2D Capon algorithm (marked in red in Fig. 7a). In case of the 1D Capon algorithm, the subarray size is 1×10 (marked in green in Fig. 7b).

After selecting the subarray, several samples are generated. Each sample is a part of the received signal corresponding to the shifted copies of the selected subarray (so-called forward spatial smoothing). The number of samples can be doubled by applying the inverse smoothing procedure [3, 5]. The spatial smoothing results in $L_{2D} = 36$ and $L_{1D} = 12 \times 6 = 72$ spatial samples for the 2D and 1D Capon algorithms, respectively.

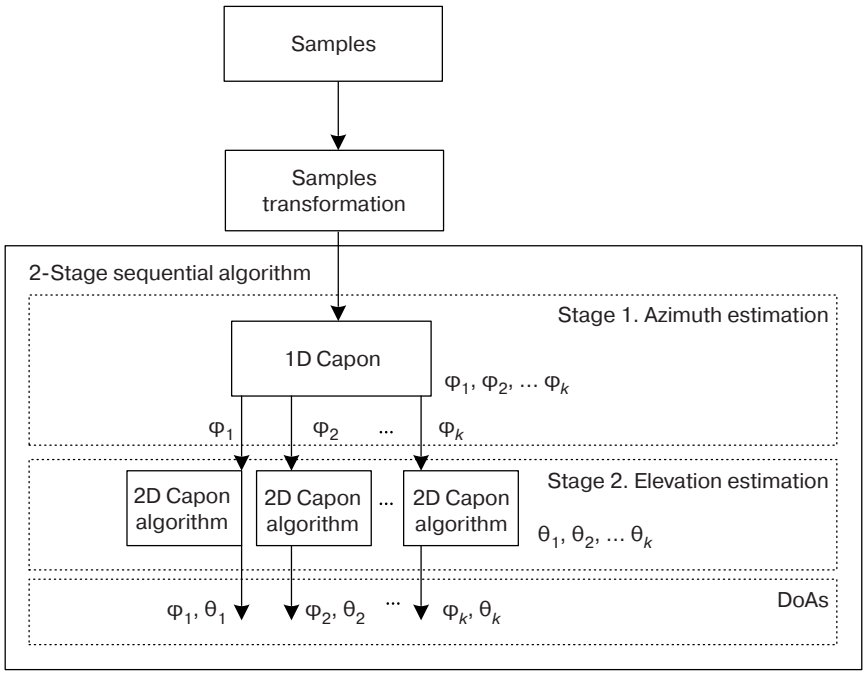

Fig. 6. Sequential algorithm for DoA estimation

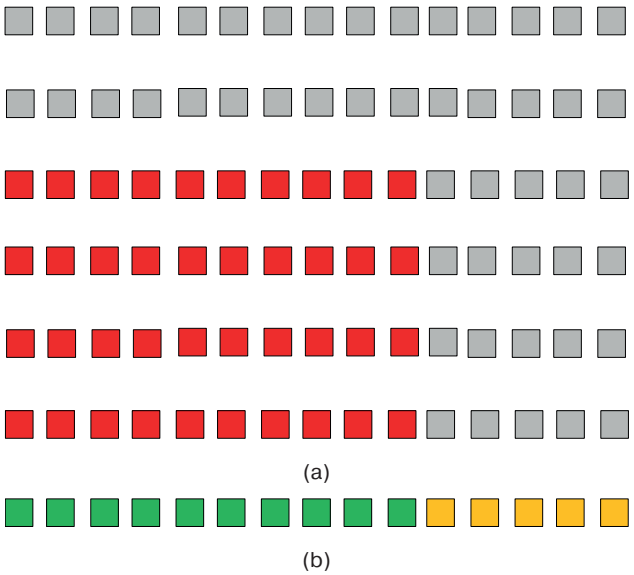

Fig. 7. Subarray configuration:
(a) subarray for the 2D Capon algorithm;
(b) subarray for the 1D Capon algorithm

2.4. Estimating computational resources

For estimating the required computational resources in the hardware implementation of algorithms, only the complex multiplication operation is considered as the costliest procedure [15, 16]. The computational complexity of the full 2D Capon method is presented in Tables 1, 2. The computational resource estimation for the proposed sequential DoA estimation algorithm is collected in Tables 3, 4.

The numerical estimates of computational resources are presented in Tables 2, 4 for the following case:

- AAS of a single *L*-type 6T8R radar;
- virtual array size (bistatic measurements): 6 × 15;
- a single snapshot;
- spatial smoothing procedure is applied.

The parameters "number of antenna elements" and "number of time samples" in Tables 2 and 4 are parameters after the spatial smoothing procedure.

Table 1. Computational costs of the 2D Capon method

Procedure	Number of operations
Estimation of the correlation matrix	$L_{2D}(N_{2D})^2 + (N_{2D})^2$
Matrix inversion	$4(N_{2D})^2$
Angles scan (Capon resolving function)	$(N_{2D})^2 + N_{2D}$
Search for maxima	$4J_1N_{steps}$
Total complexity	$(N_{2D})^2(L_{2D}+6) + N_{2D} + 4J_1N_{steps}$

Table 2. Computational cost of the 2D Capon method

Parameter	Value
Number of antenna elements	$N_{2D} = 40$
Number of time samples	$L_{2D} = 36$
Number of targets	$J_1 = 2$
Number of steps (points) to find maxima	$N_{steps} = N_hN_v$, $N_h = N_v = 100$
Total complexity	147240

Table 3. Computational cost of the sequential DoA estimation algorithm

Procedure	Number of operations
Stage 1 (1D Capon)	
Estimation of the correlation matrix	$L_{1D}(N_{1D})^2 + (N_{1D})^2$
Matrix inversion	$4(N_{1D})^2$
Scanning by resolution function angles	$(N_{1D})^2 + N_{1D}$
Search for maxima	$4J_1N_h$
Stage 2 (2D Capon)	
Estimation of the correlation matrix	$4(L_{2D}(N_{2D})^2 + (N_{2D})^2)$
Matrix inversion	$4(N_{2D})^2$
Angles scan (Capon resolving function)	$(N_{2D})^2 + N_{2D}$
Search for maxima	$2 \cdot 4J_2N_v$
Total complexity	$(N_{2D})^2(L_{2D}+6) + N_{2D} + 2 \cdot 4J_2N_v + + (N_{1D})^2(L_{2D}+6) + N_{1D} + 4J_1N_h$

Table 4. Computational cost of the sequential DoA estimation algorithm

Parameter	Value
Number of antenna elements	$N_{1D} = 10$
Number of time samples	$L_{1D} = 72$
Number of targets	$J_2 = 1$
Total complexity	76650

The computational complexity of the full 2D Capon method is 147240 operations (complex multiplications) and 76650 operations per the sequential DoA estimation algorithm for given parameters. Thus, the computational resource gain of the proposed algorithm is 1.9 times higher as compared to the classical 2D Capon algorithm.

3. NUMERICAL SIMULATION RESULTS

We assume that the distributed system consists of two coherent millimeter-wave (77 GHz) radars, the sensor spacing is 1.48 m, and the installment angle is 0° (forward-facing radars). The antenna array system of the single radar has the *L*-shaped 6T8R configuration shown in Fig. 8.

The AAS period is 0.575λ (horizontal plane) and 1.93λ (vertical plane). The single radar parameters provide FoV of ±60° in the azimuth plane and ±15° in the vertical plane. The main beam width at half power level (−3 dB) is 11.25° in the horizontal plane and 4.46° in the vertical plane.

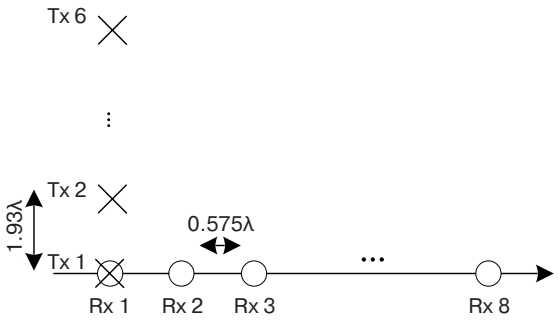

Fig. 8. AAS of the single *L*-type 6T8R radar

For the DRS, given the resulting virtual bistatic AAS, the main beam width in the vertical plane does not change; however, it decreases to ≈6° in the horizontal plane compared to a single radar.

In order to illustrate the efficiency of the distributed coherent radar system, two scenarios for spatial arrangement of two close targets are considered. In the first scenario shown in Fig. 9a, two targets are located symmetrically with respect to the *x*-axis with angular distance of 1° in the azimuth plane sharing the same elevation of 0°. The angular distance between the targets is 11 times smaller than the AAS beam width of the single radar. In the second scenario (Fig. 9b), the two targets have the same azimuth of 0° and are located symmetrically with respect to the *x*-axis in the vertical plane with an angular distance of 2°. The general arrangement of targets and radars is shown in Fig. 9c. The angular distance between targets is approximately 2.2 times smaller than the AAS beam width of a single radar in the vertical plane.

The full 2D Capon method for a single radar and the distributed system is used as the baseline algorithm for comparison with the proposed algorithm for sequential azimuth and elevation estimation for the distributed radar system (DRS). For DoA estimation, a single snapshot is taken.

The efficiency of the algorithms is compared using the Monte Carlo method. For each SNR value, a statistical ensemble of 2000 experiments is generated. Here, three main metrics are considered as functions of the SNR parameter:

1. The probability of correctly estimating the number of close targets *p*:

$$p = \frac{m}{n}, \tag{13}$$

where *m* is the number of experiments with correctly detected number of targets, while *n* is the total number of experiments.

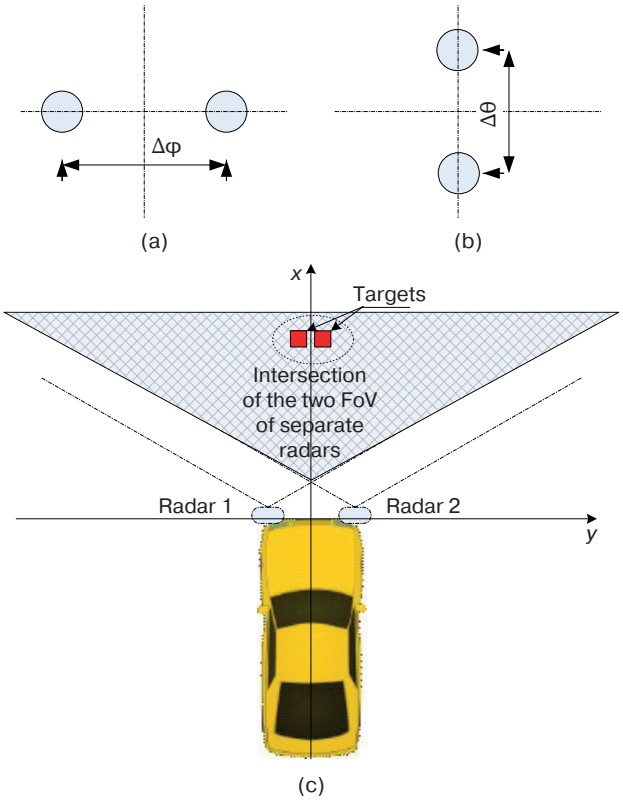

Fig. 9. Spatial arrangement scenarios for two close targets:
(a) scenario 1; (b) scenario 2; (c) general geometry of the distributed system consisting of two radars

2. The mean square error (MSE) is the following:

$$MSE = \sqrt{\frac{1}{J}\sum_{k=1}^{J}\sigma_k^2},$$
$$\sigma_k^2 = \frac{1}{m-1}\sum_{i=1}^{m}\left(\hat{\varphi}_{ki} - \bar{\varphi}_k\right)^2,\ \bar{\varphi}_k = \frac{1}{m}\sum_{i=1}^{m}\hat{\varphi}_{ki}, \quad (14)$$

where $\hat{\varphi}_{km}$ is DoA estimate for the kth target in the mth experiment.

3. The systematic error (SE) is the following:

$$SE = \sqrt{\frac{1}{J}\sum_{k=1}^{J}\left(\bar{\varphi}_k - \varphi_k\right)^2}. \quad (15)$$

The generalized numerical simulation results for the proposed algorithm of sequential azimuth and elevation estimation are presented in Table 5. It can be seen that azimuth and elevation resolutions (1° and 2°, respectively) are achieved at SNR of 36 dB (scenario 1) and 20 dB (scenario 2) for the probability of estimating the number of targets equal to 0.5 correctly.

The comparison of metrics as functions of the SNR parameter for the considered algorithms under different scenarios is shown in Figs. 10 and 11. The full set of metrics under study consists of five graphs. The left part presents MSE and SE metrics as a function of SNR for azimuth estimation, while the right part presents that for elevation estimation. The MSE and SE metrics are presented making allowance for an additional constraint on the probability of detecting correctly the number of close targets ($p > 0.5$).

Table 5. Generalized numerical simulation results for the proposed algorithm of sequential azimuth and elevation estimation

Scenario	Resolution		Accuracy		SNR
	Azimuth, Δφ	Elevation, Δθ	Azimuth	Elevation	
1	1°	–	0.12° (MSE) 0.11° (SE)	0.6° (MSE) 0.04° (SE)	36 dB
2	–	2°	0.08° (MSE) 0.02° (SE)	0.45° (MSE) 0.04° (SE)	20 dB

Scenario 1 (Fig. 9a): two targets have azimuths ±0.5° and the same elevation of 0°.

The black dashed curve with asterisks corresponds to the proposed sequential algorithm for DRS; the black dashed curve with circles corresponds to DRS for the full 2D Capon algorithm; the blue curve with triangles/red curve with crosses is the DoA estimation for the single radar (left/right); the full 2D Capon algorithm is used. It can be seen from the graphs that the single radars have failed to reach the target metric level of correctly estimating the number of targets at $p = 0.5$. Thus, the results for SNR/SE metrics are not available in graphs.

The simulation results for the current scenario show that the proposed algorithm for sequential DoA estimation outperforms the full 2D Capon algorithm in terms of metrics for correctly estimating the number of targets (for large SNR values) and MSE due to the larger number of spatial samples during azimuth estimation at the first stage (72 *vs* 36, see Section 2.4). At the same time, SE metrics for two algorithms have close values.

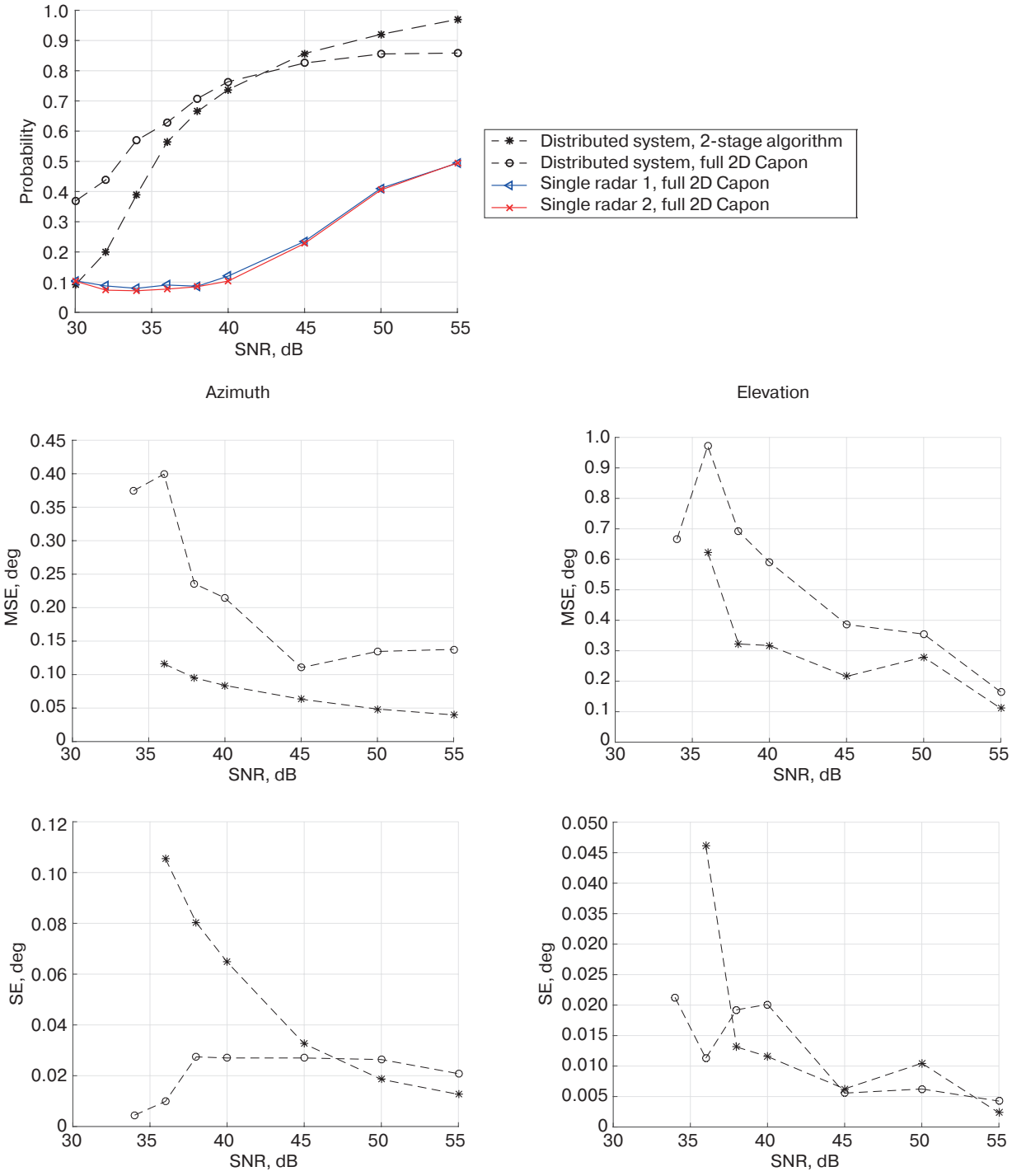

Fig. 10. Metrics as a function of SNR. Scenario 1

Scenario 2 (Fig. 9b): two targets have the same azimuth of 0° and elevation of ±1° (angular distance of 2° in the vertical plane).

The results of the study show that the sequential algorithm for estimating directions of arrival leads to an improvement in SNR and SE metrics. While a single radar can also distinguish between two close targets in Scenario 2 due to the same apertures of AASs of the single radar and the distributed system in the vertical plane, the single radar with the full 2D Capon algorithm loses in SNR and SE metrics to DRS with the two-step algorithm.

The advantage of the proposed algorithm for DoA sequential estimation compared to the full 2D Capon algorithm can be explained by a more accurate azimuth estimation at the first stage of the method due to a larger number of spatial samples (72 *vs* 36), while the classical 2D Capon algorithm is compelled to estimate azimuth and elevation simultaneously with a shorter spatial sample length.

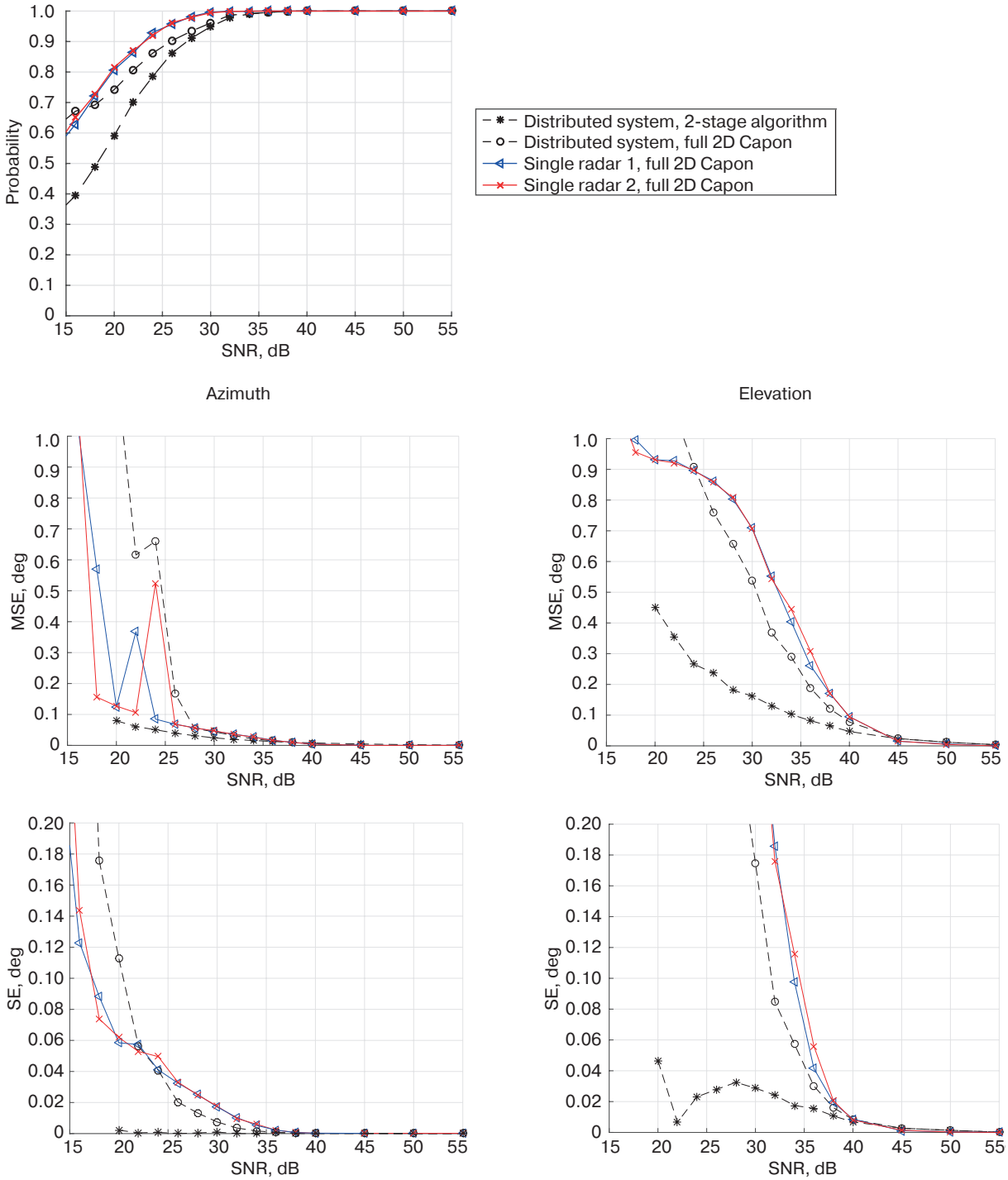

Fig. 11. Metrics as a function of SNR. Scenario 2

CONCLUSIONS

A two-dimensional method for estimating directions of arrival in azimuth and elevation planes for the distributed system of bistatic coherent MIMO-radars has been proposed. The method, which is based on the sequential estimation of DoAs (in the azimuth plane at the first stage and in the elevation plane at the second stage), ensures 1.9 times gain (at selected system parameters) in terms of use of computational resources as compared to the full classical 2D Capon method.

The comparative numerical simulation based on the Monte-Carlo method shows that the proposed scheme for coherent processing of distributed radar signals for DoA estimation leads to an improvement in target metrics (probability of correctly estimating the number of targets, MSE and SE) compared to a single radar. The performance of the system comprising coherent radars having a limited AAS configuration is comparable to that of a high-performance 4D radar with a much larger number of AAS elements.

REFERENCES

1. Giannini V., Goldenberg M., Eshrahi A., et al. 9.2 A 192-Virtual-Receiver 77/79GHz GMSK Code-Domain MIMO Radar System-on-Chip. In: *2019 IEEE International Solid-State Circuits Conference* (*ISSCC*), San Francisco, CA, USA. 2019. P. 164–166. https://doi.org/10.1109/ISSCC.2019.8662386
2. Godara L.C. *Smart Antennas*. CRC Press; 2004. 472 p.
3. Tuncer T.E., Friedlander B. (Eds.). *Classical and Modern Direction-of-Arrival Estimation*. Academic Press, Inc.; 2009. 456 p. https://doi.org/10.1016/C2009-0-19135-3
4. Ermolaev V.T., Flaksman A.G., Elokhin A.V., et al. Minimal Polynomial Method for Estimating Parameters of Signals Received by an Antenna Array. *Acoust. Phys.* 2018;64(1):83–90. https://doi.org/10.1134/S1063771018010050
   [Original Russian Text: Ermolaev V.T., Flaksman A.G., Elokhin A.V., Kuptsov V.V. Minimal Polynomial Method for Estimating Parameters of Signals Received by an Antenna Array. *Akusticheskii Zhurnal*. 2018;64(1):78–85 (in Russ.). https://doi.org/10.7868/S0320791918010057]
5. Ermolaev V.T., Flaksman A.G., Elokhin A.V., et al. Angular Superresolution of the Antenna-Array Signals Using the Root Method of Minimum Polynomial of the Correlation Matrix. *Radiophys. Quantum Electron*. 2018;61(3):232–241. https://doi.org/10.1007/s11141-018-9884-5
   [Original Russian Text: Ermolaev V.T., Flaksman A.G., Elokhin A.V., Shmonin O.A. Angular Superresolution of the Antenna-Array Signals Using the Root Method of Minimum Polynomial of the Correlation Matrix. *Izvestiya Vysshikh Uchebnykh Zavedenii. Radiofizika*. 2018;61(3):261–272 (in Russ.).]
6. Rodionov A.A., Turchin V.I. Processing of Antenna-Array Signals on the Basis of the Interference Model Including a Rank-Deficient Correlation Matrix. *Radiophys. Quantum Electron*. 2017;60(1):54–64. https://doi.org/10.1007/s11141-017-9776-0
   [Original Russian Text: Rodionov A.A., Turchin V.I. Processing of Antenna-Array Signals on the Basis of the Interference Model Including a Rank-Deficient Correlation Matrix. *Izvestiya Vysshikh Uchebnykh Zavedenii. Radiofizika*. 2017;60(1):60–71 (in Russ.).]
7. Patole S.M., Torlak M., Wang D., Ali M. Automotive radars: A review of signal processing techniques. *IEEE Signal Processing Magazine.* 2017;34(2):22–35. https://doi.org/10.1109/MSP.2016.2628914
8. Ermolaev V.T., Semenov V.Yu., Flaksman A.G., Artyukhin I.V., Shmonin O.A. The method of forming virtual receiving channels in the automobile MIMO-radar. *Radiotekhnika = J. Radioengineering*. 2021;85(7):115–126 (in Russ.).
9. Li J., Stoica P. *MIMO Radar Signal Processing*. Wiley-IEEE Press; 2009. 448 p. ISBN 978-0-4701-7898-0
10. Folster F., Rohling H., Lubbert U. An automotive radar network based on 77 GHz FMCW sensors. In: *IEEE International Radar Conference*. 2005. P. 871–876. https://doi.org/10.1109/RADAR.2005.1435950
11. Artyukhin I.V., Averin I.M., Flaksman A.G., Rubtsov A.E. Direction-of-Arrival Estimation Algorithm in Automotive Distributed Non-Coherent Multi-Radar Systems. *Zhurnal radioelektroniki = J. Radio Electronics*. 2023;4:1–20 (in Russ.). https://doi.org/10.30898/1684-1719.2023.4.2
12. Gottinger M., Hoffmann M., Christmann M., Schutz M., Kirsch F., Gulden P., Vossiek M. Coherent Automotive Radar Networks: The Next Generation of Radar-Based Imaging and Mapping. *IEEE Journal of Microwaves*. 2021;1(1):149–163. https://doi.org/10.1109/JMW.2020.3034475
13. Richards M.A. *Fundamentals of Radar Signal Processing*. 2nd edition. New York: McGraw-Hill; 2014. 656 p.
14. Ermolaev V.T., Flaksman A.G., Shmonin O.A. Using the Concept of a Virtual Antenna Array in a MIMO Radar in the Presence of Reflections from the Ground Surface. *Radiophys. Quantum Electron*. 2020;63(3):218–226. https://doi.org/10.1007/s11141-021-10047-1
    [Original Russian Text: Ermolaev V.T., Flaksman A.G., Shmonin O.A. Using the Concept of a Virtual Antenna Array in a MIMO Radar in the Presence of Reflections from the Ground Surface. *Izvestiya Vysshikh Uchebnykh Zavedenii. Radiofizika*. 2020;63(3):240–249(in Russ.).]
15. Björnson E., Hoydis J., Sanguinetti L. Massive MIMO Networks: Spectral, Energy, and Hardware Efficiency. *Foundations and Trends® in Signal Processing.* 2017;11(3–4):154–655. http://doi.org/10.1561/2000000093
16. Gentilho E., Scalassara P.R., Abrão T. Direction-of-Arrival Estimation Methods: A Performance-Complexity Tradeoff Perspective. *J. Sign. Process. Syst.* 2020;92(2):239–256. https://doi.org/10.1007/s11265-019-01467-4

СПИСОК ЛИТЕРАТУРЫ

1. Giannini V., Goldenberg M., Eshrahi A., et al. 9.2 A 192-Virtual-Receiver 77/79GHz GMSK Code-Domain MIMO Radar System-on-Chip. In: *2019 IEEE International Solid-State Circuits Conference* (*ISSCC*), San Francisco, CA, USA. 2019. P. 164–166. https://doi.org/10.1109/ISSCC.2019.8662386
2. Godara L.C. *Smart Antennas*. CRC Press; 2004. 472 p.
3. Tuncer T.E., Friedlander B. (Eds.). *Classical and Modern Direction-of-Arrival Estimation*. Academic Press, Inc.; 2009. 456 p. https://doi.org/10.1016/C2009-0-19135-3
4. Ермолаев В.Т., Флаксман А.Г., Елохин А.В., Купцов В.В. Метод минимального многочлена для оценки параметров сигналов, принимаемых антенной решеткой. *Акустический журнал*. 2018;64(1):78–85. https://doi.org/10.7868/S0320791918010057
5. Ермолаев В.Т., Флаксман А.Г., Елохин А.В., Шмонин О.А. Угловое сверхразрешение сигналов в антенной решетке с помощью корневого метода минимального многочлена корреляционной матрицы. *Известия вузов. Радиофизика*. 2018;61(3):261–272.
6. Родионов А.А., Турчин В.И. Обработка сигналов в антенных решётках на основе модели помехи, включающей корреляционную матрицу неполного ранга. *Известия вузов. Радиофизика*. 2017;60(1):60–71.
7. Patole S.M., Torlak M., Wang D., Ali M. Automotive radars: A review of signal processing techniques. *IEEE Signal Processing Magazine.* 2017;34(2):22–35. https://doi.org/10.1109/MSP.2016.2628914
8. Ермолаев В.Т., Семенов В.Ю., Флаксман А.Г., Артюхин И.В., Шмонин О.А. Метод формирования виртуальных приемных каналов в автомобильном MIMO-радаре. *Радиотехника*. 2021;85(7):115–126.
9. Li J., Stoica P. *MIMO Radar Signal Processing*. Wiley-IEEE Press; 2009. 448 p. ISBN 978-0-4701-7898-0
10. Folster F., Rohling H., Lubbert U. An automotive radar network based on 77 GHz FMCW sensors. In: *IEEE International Radar Conference*. 2005. P. 871–876. https://doi.org/10.1109/RADAR.2005.1435950
11. Артюхин И.В., Аверин И.М., Флаксман А.Г., Рубцов А.Е. Алгоритм оценки углов прихода сигналов в системе распределенных некогерентных автомобильных радаров. *Журнал радиоэлектроники*. 2023;4:1–20. http://jre.cplire.ru/jre/apr23/2/text.pdf
12. Gottinger M., Hoffmann M., Christmann M., Schutz M., Kirsch F., Gulden P., Vossiek M. Coherent Automotive Radar Networks: The Next Generation of Radar-Based Imaging and Mapping. *IEEE Journal of Microwaves*. 2021;1(1):149–163. https://doi.org/10.1109/JMW.2020.3034475
13. Richards M.A. *Fundamentals of Radar Signal Processing*. 2nd edition. New York: McGraw-Hill; 2014. 656 p.
14. Ермолаев В.Т., Флаксман А.Г., Шмонин О.А. Применение концепции виртуальной антенной решетки в MIMO-радаре при наличии отражений от земной поверхности. *Известия вузов. Радиофизика*. 2020;63(3):240–249.
15. Björnson E., Hoydis J., Sanguinetti L. Massive MIMO Networks: Spectral, Energy, and Hardware Efficiency. *Found. Trends® Sign. Process.* 2017;11(3–4):154–655. http://doi.org/10.1561/2000000093
16. Gentilho E., Scalassara P.R., Abrão T. Direction-of-Arrival Estimation Methods: A Performance-Complexity Tradeoff Perspective. *J. Sign. Process. Syst.* 2020;92(2):239–256. https://doi.org/10.1007/s11265-019-01467-4

About the author

Igor V. Artyukhin, Engineer, Department of Statistical Radiophysics and Mobile Communication Systems, Faculty of Radiophysics, National Research Lobachevsky State University of Nizhny Novgorod (23, Gagarina pr., Nizhny Novgorod, 603022 Russia). E-mail: artjukhin@rf.unn.ru. Scopus Author ID 57216223873, https://orcid.org/0009-0008-5139-6443

Об авторе

Артюхин Игорь Владимирович, электроник 1 категории, кафедра статистической радиофизики и мобильных систем связи, Радиофизический факультет, ФГАОУ ВО «Национальный исследовательский Нижегородский государственный университет им. Н.И. Лобачевского» (603022, Россия, Нижний Новгород, пр-т Гагарина, д. 23). E-mail: artjukhin@rf.unn.ru. Scopus Author ID 57216223873, https://orcid.org/0009-0008-5139-6443

Translated from Russian into English by K. Nazarov
Edited for English language and spelling by Thomas A. Beavitt